AMERICAN SOCIETY FOR MICROBIOLOGY | Applied and Environmental Microbiology®

PHYSIOLOGY

Proteins Encoded by the *gerP* Operon Are Localized to the Inner Coat in *Bacillus cereus* Spores and Are Dependent on GerPA and SafA for Assembly

Abhinaba Ghosh,[a] James D. Manton,[a] Amin R. Mustafa,[a] Mudit Gupta,[a] Alejandro Ayuso-Garcia,[a] Eric J. Rees,[a] Graham Christie[a]

[a]Department of Chemical Engineering and Biotechnology, University of Cambridge, Cambridge, United Kingdom

ABSTRACT The germination of *Bacillus* spores is triggered by certain amino acids and sugar molecules which permeate the outermost layers of the spore to interact with receptor complexes that reside in the inner membrane. Previous studies have shown that mutations in the hexacistronic *gerP* locus reduce the rate of spore germination, with experimental evidence indicating that the defect stems from reduced permeability of the spore coat to germinant molecules. Here, we use the ellipsoid localization microscopy technique to reveal that all six *Bacillus cereus* GerP proteins share proximity with cortex-lytic enzymes within the inner coat. We also reveal that the GerPA protein alone can localize in the absence of all other GerP proteins and that it has an essential role for the localization of all other GerP proteins within the spore. Its essential role is also demonstrated to be dependent on SafA, but not CotE, for localization, which is consistent with an inner coat location. GerP-null spores are shown also to have reduced permeability to fluorescently labeled dextran molecules compared to wild-type spores. Overall, the results support the hypothesis that the GerP proteins have a structural role within the spore associated with coat permeability.

IMPORTANCE The bacterial spore coat comprises a multilayered proteinaceous structure that influences the distribution, survival, and germination properties of spores in the environment. The results from the current study are significant since they increase our understanding of coat assembly and architecture while adding detail to existing models of germination. We demonstrate also that the ellipsoid localization microscopy (ELM) image analysis technique can be used as a novel tool to provide direct quantitative measurements of spore coat permeability. Progress in all of these areas should ultimately facilitate improved methods of spore control in a range of industrial, health care, and environmental sectors.

KEYWORDS *Bacillus*, spore, coat, germination, permeability, spore coat, spores

Bacterial endospores (here, spores) are ubiquitous in the environment. They are formed by members of the *Bacillales* and *Clostridiales* orders in response to nutrient starvation, with *Bacillales* being aerobic species and *Clostridiales* being anaerobes. Their ubiquity results from the protective cellular structure that the spore displays, as shown in Fig. 1. This comprises a central protoplast, or core, which is enveloped, consecutively, by an inner membrane, notable for the reduced fluidity of its lipids, and a thick layer of peptidoglycan, which itself can be subdivided into a structurally distinct germ cell wall and cortex (1). A second membrane, which may be discontinuous, surrounds the cortex, followed by a multilayered coat composed of numerous different proteins. Finally, in some species, the coat itself is surrounded by an outermost structure referred to as the exosporium (2). The various structural features have different primary func-

Received 2 April 2018 **Accepted** 24 April 2018

Accepted manuscript posted online 4 May 2018

Citation Ghosh A, Manton JD, Mustafa AR, Gupta M, Ayuso-Garcia A, Rees EJ, Christie G. 2018. Proteins encoded by the *gerP* operon are localized to the inner coat in *Bacillus cereus* spores and are dependent on GerPA and SafA for assembly. Appl Environ Microbiol 84:e00760-18. https://doi.org/10.1128/AEM.00760-18.

Editor Claire Vieille, Michigan State University

Address correspondence to Graham Christie, gc301@cam.ac.uk.

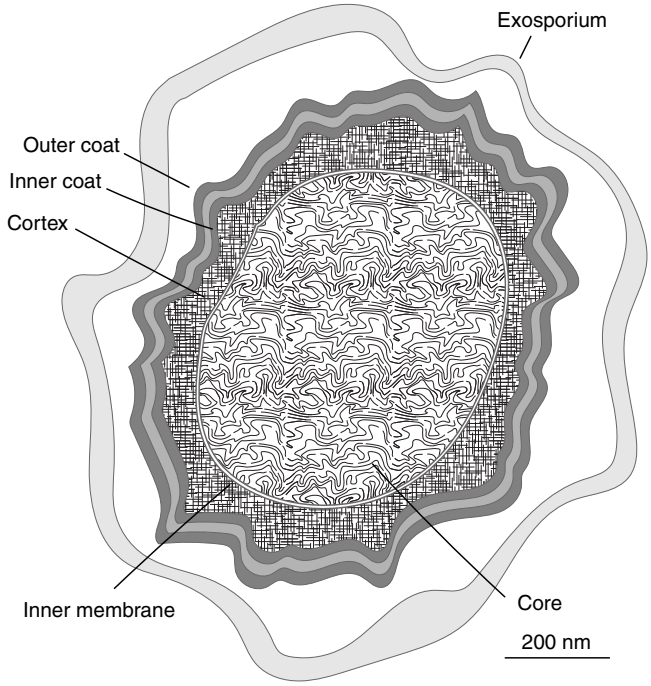

FIG 1 Schematic of a bacterial spore. The major cellular structures evident in thin-section transmission electron microscopy images are shown. The spore coat can typically be subdivided into outer and inner coat structures, with the pattern of striation depending on the species. The exosporium is present in some species, including *B. cereus*, but is absent in others, including *B. subtilis*.

tions. The coat, for example, protects against degradative enzymes and harmful chemicals (3), whereas the cortex, in conjunction with unique core metabolites, such as dipicolinic acid (DPA), results in a protoplast of sufficiently low water activity to ensure metabolic dormancy (4). In this state, bacterial spores can persist in a dormant state in the environment for extended periods of time.

In order to resume the vegetative cell cycle, the spore must respond to environmental cues that indicate that conditions are once again conducive to growth, all the while being dormant and encased in a multilayered protective shell. The spore-sensing system comprises receptor proteins that are localized to the inner membrane, which respond typically to various amino acids, monosaccharides, and inorganic ions (5). Combinations of these germinant molecules are often required to stimulate efficient germinative responses. In spores of *Bacillus* species, presumed binding of germinants to receptor proteins results in the release of dipicolinic acid chelated with Ca^{2+} ions (CaDPA) and other small molecules from the spore core, followed by the activation of specialized lysins that degrade the cortical peptidoglycan. These activities permit hydration of the protoplast, resumption of metabolism, and, concomitant with shedding of the coat, the emergence of a new vegetative cell (5).

A degree of permeability in the spore structure is therefore required to permit the transit of small-molecule germinants through the various integument layers to reach and interact with the germinant receptors. In this context, proteins encoded by the hexacistronic *gerP* operon, which is present in the genomes of all *Bacillus* species, have been implicated in having a role in maintaining the permeability of the spore coat. This stems from work conducted initially in *Bacillus cereus* 569, in which spores with a transposon insertion in the operon had a germination defect that could be relieved by chemical removal of the coat (6). Subsequent mutagenesis analyses with *Bacillus subtilis* (7) and *Bacillus anthracis* (8) spores revealed that they too have defective germination phenotypes when the *gerP* operon is disrupted, or in the case of the *B. anthracis*, when individual *gerP* genes are deleted. However, other than being required for efficient spore germination and a suggestion that they are probably coat proteins, little is known

of the GerP proteins. Bioinformatic analyses do not reveal any functional clues, only that the various GerP proteins largely resemble orthologous proteins in other *Bacillus* species. Hence, the purpose of the current study was to use the recently developed ellipsoid localization microscopy (ELM) technique (9) to more precisely determine the location of the various GerP proteins in *Bacillus cereus* spores. We sought additionally to ascertain whether there is any dependency between the various GerP proteins, and between the GerP and coat morphogenetic proteins, for localization in the spore. Finally, ELM was used to directly assess the permeabilities of *gerP* spores to fluorescently labeled dextran molecules compared to wild-type spores.

RESULTS

Construction and germination of *B. cereus* 14579 *gerP* strains. Defective spore germination phenotypes associated with the *gerP* operon were first observed in *Bacillus cereus* strain 569 bearing a transposon (Tn*917*) insertion between *gerPB* and *gerPC* (6). Our initial attempts at creating markerless deletions of the entire *gerP* operon and individual genes within the operon in this strain proved to be unsuccessful. Accordingly, the decision was made to switch the work to *B. cereus* 14579, which appears to be more amenable to genetic manipulation. A markerless allelic exchange system was subsequently used to create a series of strains in the 14579 background where individual genes (start and stop codons aside) from *gerPA* through *gerPF* were deleted (Table 1; see also Table S1 and Fig. S1 in the supplemental material). The same markerless approach was used to delete the entire *gerP* operon, with the exception of the start codon from *gerPA* and the stop codon of *gerPF* (strain AG007). In common with *B. subtilis* and *B. anthracis*, *B. cereus* 14579 has two additional *gerPF* homologues on the chromosome (BC2276 and BC4794; Table S2), although these were not deleted in the course of this work. Analysis of the resultant null mutant spores by transmission electron microscopy revealed no obvious morphological defects compared to wild-type spores (Fig. S2).

In order to assess whether the deletion of individual or collective *gerP* genes resulted in defective germination phenotypes in the *B. cereus* 14579 background, spores of the various null strains were subjected to a heat shock of 70°C for 15 min and cooled on ice, and their germinative responses to L-alanine and inosine were assessed by monitoring the reduction in absorbance associated with the transition of phase-bright dormant spores to phase-dark germinated spores. Spores of all strains, apart from the *gerPF* null strain, were defective for germination in buffer supplemented with either alanine or inosine with respect to wild-type spores (Fig. 2, S3, and S4). The slight reduction in absorbance recorded after 5 min of germination of mutant spores appeared to be associated with the germination of a small number of spores within the various populations, at least as judged by the light microscope. In contrast, the majority of wild-type spores were phase gray or phase dark after 5 min (data not shown). Even after 60 min, the total loss of absorbance was less than that associated with wild-type spores, with microscopy revealing again the presence of many refractile dormant spores in the mutant populations. In all cases, germination defects were restored by complementation with plasmid-borne copies of the deleted gene(s) (Fig. S4). In contrast to the above-mentioned observations, the *gerPF* spore germinative responses to alanine and inosine were indistinguishable from those of wild-type spores, indicating that the homologous genes encoded elsewhere on the chromosome can compensate for the loss of *gerPF*. Additionally, the viability of the various *gerP* null spores was reduced when incubated overnight on rich solid medium, with colony counts for all mutant spores typically at 20% of those obtained when plating comparable quantities of wild-type spores (data not shown).

Spores can also be stimulated to germinate by various nonphysiological routes, including by exposure to high concentrations of dipicolinic acid chelated with Ca^{2+} ions (CaDPA) and to the cationic detergent dodecylamine (5). In order to assess the impact of deletion of the various GerP proteins in *B. cereus* 14579 on germination via these routes, spores of the various strains were prepared and incubated in CaDPA or

TABLE 1 *Bacillus* strains used in this study

Strain	Relevant phenotype or genotype[a]	Source or reference
B. subtilis strains		
PS832	Wild type	Peter Setlow
PS4228	Δ*gerP* Tc^r	Peter Setlow
B. cereus strains		
14579	Wild type	Toril Lindbäck
AG001	Δ*gerPA*	This study
AG002	Δ*gerPB*	This study
AG003	Δ*gerPC*	This study
AG004	Δ*gerPD*	This study
AG005	Δ*gerPE*	This Study
AG006	Δ*gerPF*	This study
AG007	Δ*gerP*	This study
AM001	Δ*spoIVA*	This study
AM002	Δ*safA*	This study
AM003	Δ*cotE*	This study
Mutant transformants		
AG008	Δ*gerPA*::pHT315-promoter-*gerPA* MLS^r	This study
AG009	Δ*gerPB*::pHT315-promoter-*gerPB* MLS^r	This study
AG010	Δ*gerPC*::pHT315-promoter-*gerPC* MLS^r	This study
AG011	Δ*gerPD*::pHT315-promoter-*gerPD* MLS^r	This study
AG012	Δ*gerPE*::pHT315-promoter-*gerPE* MLS^r	This study
AG013	Δ*gerPF*::pHT315-promoter-*gerPF* MLS^r	This study
AG014	Δ*gerP*::pHT315-promoter-*gerP* MLS^r	This study
GerP localization strains		
AG015	pHT315-promoter-*PA-gfp-PB-PC-PD-PE-PF* MLS^r	This study
AG016	pHT315-promoter-*PA-PB-gfp-PC-PD-PE-PF* MLS^r	This study
AG017	pHT315-promoter-*PA-PB-PC-gfp-PD-PE-PF* MLS^r	This study
AG018	pHT315-promoter-*PA-PB-PC-PD-gfp-PE-PF* MLS^r	This study
AG019	pHT315-promoter-*PA- PB-PC-PD-PE-gfp-PF* MLS^r	This study
AG020	pHT315-promoter-*PA-PB-PC-PD-PE–PF-gfp* MLS^r	This study
Dependency studies		
AM004	Δ*spoIVA*::pHT315-promoter-*gerPA-gfp* MLS^r	This study
AM005	Δ*safA*::pHT315-promoter-*gerPA-gfp* MLS^r	This study
AM006	Δ*cotE*::pHT315-promoter-*gerPA* MLS^r	This study
AG022	Δ*gerPA*::pHT315-promoter-*gerPA-gfp* MLS^r	This study
AG023	Δ*gerPA*::pHT315-promoter-*gerPB-gfp* MLS^r	This study
AG024	Δ*gerPA*::pHT315-promoter-*gerPC-gfp* MLS^r	This study
AG025	Δ*gerPA*::pHT315-promoter-*gerPD-gfp* MLS^r	This study
AG026	Δ*gerPA*::pHT315-promoter-*gerPE-gfp* MLS^r	This study
AG027	Δ*gerPA*::pHT315-promoter-*gerPF-gfp* MLS^r	This study
AG028	Δ*gerPB*::pHT315-promoter-*gerPA-gfp* MLS^r	This study
AG029	Δ*gerPB*::pHT315-promoter-*gerPB-gfp* MLS^r	This study
AG030	Δ*gerPB*::pHT315-promoter-*gerPC-gfp* MLS^r	This study
AG031	Δ*gerPB*::pHT315-promoter-*gerPD-gfp* MLS^r	This study
AG032	Δ*gerPB*::pHT315-promoter-*gerPE-gfp* MLS^r	This study
AG033	Δ*gerPB*::pHT315-promoter-*gerPF-gfp* MLS^r	This study
AG034	Δ*gerPC*::pHT315-promoter-*gerPA-gfp* MLS^r	This study
AG035	Δ*gerPC*::pHT315-promoter-*gerPB-gfp* MLS^r	This study
AG036	Δ*gerPC*::pHT315-promoter-*gerPC-gfp* MLS^r	This study
AG037	Δ*gerPC*::pHT315-promoter-*gerPD-gfp* MLS^r	This study
AG038	Δ*gerPC*::pHT315-promoter-*gerPE-gfp* MLS^r	This study
AG039	Δ*gerPC*::pHT315-promoter-*gerPF-gfp* MLS^r	This study
AG040	Δ*gerPD*::pHT315-promoter-*gerPA-gfp* MLS^r	This study
AG041	Δ*gerPD*::pHT315-promoter-*gerPB-gfp* MLS^r	This study
AG042	Δ*gerPD*::pHT315-promoter-*gerPC-gfp* MLS^r	This study
AG043	Δ*gerPD*::pHT315-promoter-*gerPD-gfp* MLS^r	This study
AG044	Δ*gerPD*::pHT315-promoter-*gerPE-gfp* MLS^r	This study
AG045	Δ*gerPD*::pHT315-promoter-*gerPF-gfp* MLS^r	This study
AG046	Δ*gerPE*::pHT315-promoter-*gerPA-gfp* MLS^r	This study
AG047	Δ*gerPE*::pHT315-promoter-*gerPB-gfp* MLS^r	This study
AG048	Δ*gerPE*::pHT315-promoter-*gerPC-gfp* MLS^r	This study

(Continued on next page)

TABLE 1 (Continued)

Strain	Relevant phenotype or genotype[a]	Source or reference
AG049	Δ*gerPE*::pHT315-promoter-*gerPD-gfp* MLS^r	This study
AG050	Δ*gerPE*::pHT315-promoter-*gerPE-gfp* MLS^r	This study
AG051	Δ*gerPE*::pHT315-promoter-*gerPF-gfp* MLS^r	This study
AG052	Δ*gerPF*::pHT315-promoter-*gerPA-gfp* MLS^r	This study
AG053	Δ*gerPF*::pHT315-promoter-*gerPB-gfp* MLS^r	This study
AG054	Δ*gerPF*::pHT315-promoter-*gerPC-gfp* MLS^r	This study
AG055	Δ*gerPF*::pHT315-promoter-*gerPD-gfp* MLS^r	This study
AG056	Δ*gerPF*::pHT315-promoter-*gerPE-gfp* MLS^r	This study
AG057	Δ*gerPF*::pHT315-promoter-*gerPF-gfp* MLS^r	This study
AG058	Δ*gerP*::pHT315-promoter-*gerPA-gfp* MLS^r	This study
AG059	Δ*gerP*::pHT315-promoter-*gerPB-gfp* MLS^r	This study
AG060	Δ*gerP*::pHT315-promoter-*gerPC-gfp* MLS^r	This study
AG061	Δ*gerP*::pHT315-promoter-*gerPD-gfp* MLS^r	This study
AG062	Δ*gerP*::pHT315-promoter-*gerPE-gfp* MLS^r	This study
AG063	Δ*gerP*::pHT315-promoter-*gerPF-gfp* MLS^r	This study

[a]Tc^r, tetracycline resistance; MLS^r, macrolide-lincosamide-streptogramin-B resistance.

dodecylamine, and germination was monitored by measuring the absorbance loss. In all cases examined, germination was reduced compared to that observed with wild-type spores, again with the exception of the *gerPF* spores, which showed essentially wild-type germinative responses (Fig. 2 and S4). Microscopy analyses conducted at the end of each experiment revealed the spore populations to comprise a mixture of predominantly dormant (phase-bright) spores interspersed with lower numbers of germinated (phase-dark) and partially germinated (phase-gray) spores (data not shown). In contrast, wild-type spores were essentially all phase dark. Hence, for both of the nonnutrient germinative pathways examined, a minority of spores can complete germination, whereas most remain dormant.

Localization of GerP proteins. A series of strains designed to individually express each of the respective GerP proteins as C-terminal green fluorescent protein (GFP) fusion proteins were constructed using derivatives of the low-copy-number pHT315 episomal plasmid. The strategy essentially involved cloning the entire *gerP* operon plus

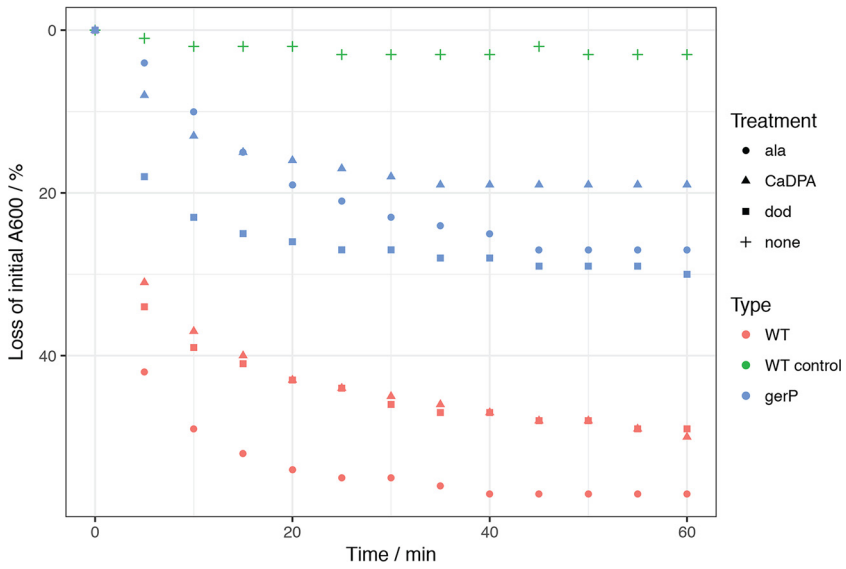

FIG 2 Germination of *B. cereus gerP* spores in response to nutrient and nonnutrient germinants. Spores at an OD_{600} of 1 were suspended in buffer supplemented with defined germinants and the resultant changes in absorbance monitored, as described in Materials and Methods. For germinants: circles, 100 mM alanine (ala) (red, wild type; blue, *gerP*); triangles, 50 mM CaDPA (red, wild type; blue, *gerP*); squares, 1 mM dodecylamine (dod) (red, wild type; blue, *gerP*). The + sign represents wild-type spores in buffer without germinant.

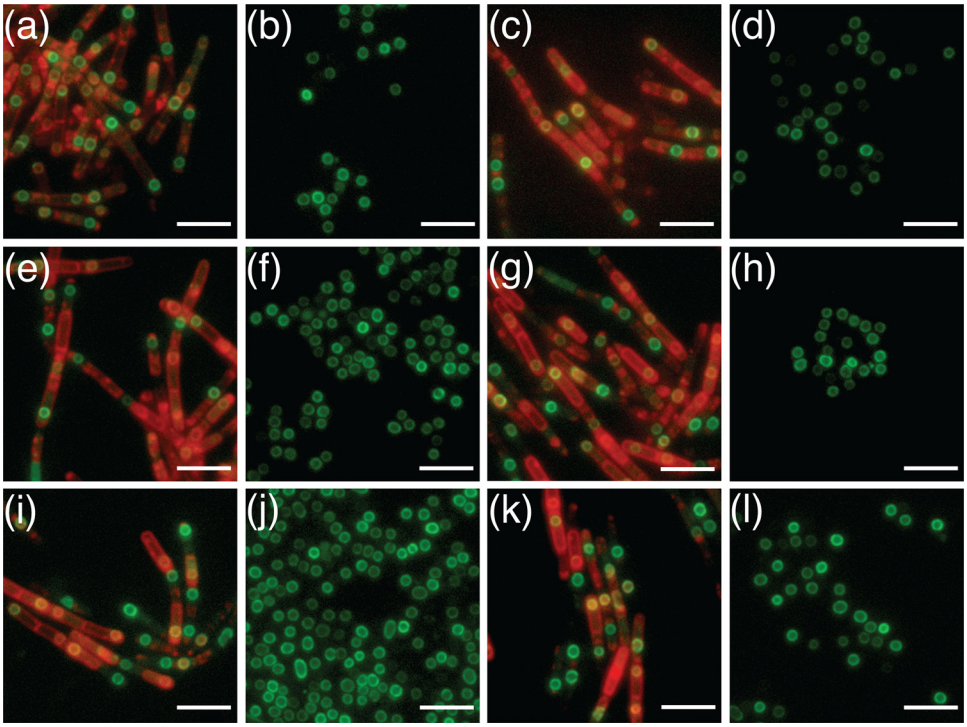

FIG 3 Fluorescence microscopy of *B. cereus* 14579 sporulating cells and spores with plasmid-borne copies of *gerPA-gfp* (a and b), *gerPB-gfp* (c and d), *gerPC-gfp* (e and f), *gerPD-gfp* (g and h), *gerPE-gfp* (i and j), and *gerPF-gfp* (k and l). The expression of various genes was controlled by native *gerP* operon regulatory sequences. Red fluorescence is associated with the lipophilic FM4-64 dye, which was used to visualize cell membranes. Scale bar = 5 μm.

regulatory sequences into pHT315 and then introducing the *gfp* gene in-frame at the 3′ end of the gene of interest (minus its stop codon). Individual plasmid constructs carrying *gerPA-gfp* through *gerPF-gfp* were subsequently introduced to wild-type cells by electroporation (Table 1), meaning that any expressed fusion proteins would be competing for presumed binding sites within the spore with native GerP proteins expressed from the chromosome. Fluorescence microscopy was used to analyze the various *gfp*-bearing strain cells at intervals throughout sporulation and to examine the final spores in order to observe the pattern of deposition of the various GerP proteins. In all cases, expression was observed first as diffuse fluorescence in the mother cell, followed by a ring of green fluorescence that developed around the still-phase-dark forespore (Fig. 3). In some developing spores, fluorescence was observed as two hemispheres separated by small junctions at either end of the forespore. Fluorescence was retained in mature spores of all strains (Fig. 3), albeit at reduced levels compared to sporulating cells, indicating that the GerP proteins are structural components of the spore rather than being associated purely with the expression or assembly of another component of the spore. Additionally, spores of the various *gfp*-bearing strains appeared to be free of any germination defects in response to both alanine and inosine (Fig. S4), indicating in all cases that the GFP moiety was not disruptive to function.

Ellipsoid localization microscopy was then used to more precisely locate the various GerP proteins in *B. cereus* spores. Information about the location and distribution of proteins in the coat and exosporium of *B. cereus* is sparse in comparison to that available for *B. subtilis* spores. However, previous studies have revealed that the BclA protein forms the fiber-like nap on the exterior surface of the exosporium (10, 11), whereas CotD has been identified as a component of the spore coat (12). Accordingly, strains bearing *gfp* fusions to the 3′ ends of these genes were constructed to serve as benchmarks for the exosporium and coat locations. Strains designed to express C-terminal GFP fusions to SleL and CwlJ were also constructed, since at least in *B.*

subtilis, these cortex-lytic enzymes have been localized to the inner coat (13). Spores of additional strains, including those with *bxpB-gfp* (BxpB is an exosporium protein [11, 14]), were prepared but failed to show any fluorescence, whereas the irregular distribution of fluorescent foci evident in *cotE-gfp* spores precluded ELM analysis. CotE is important in the assembly of spore outer coat proteins (13), and it may be that the GFP moiety disrupted its key morphogenetic role in our study.

The radial locations of the GerP proteins with respect to the spore center are shown in Fig. 4, together with the numbers of individual spores analyzed and the residual fitting error of the ELM measurements. We infer the radial location of GerPA, for example, as 454 nm ± 14 nm in mature spores, where the ±14 nm is the standard deviation of radial locations found in repeated measurements. The radial locations are as follows: GerPB, 442 nm (±23 nm); GerPC, 427 nm (±4 nm); GerPD, 407 nm (±11 nm); GerPE, 444 nm (±10 nm); and GerPF, 434 nm (±10 nm) (Fig. 4). As expected, the BclA-GFP protein was measured as having the largest equivalent radius at 566 nm (±23 nm), which is consistent with its position on the exterior of the spore. Similarly, ELM-derived measurements indicate that the CotD-GFP protein, with an equivalent radius of 484 nm (±12 nm), is located to the exterior of both SleL-GFP (456 nm ± 12 nm) and CwlJ-GFP (447 nm ± 12 nm), with the two cortex-lytic enzymes (CLEs) apparently occupying similar locations within the spore. We can infer from these data that the GerP proteins are distributed within the inner spore coat, using the CLEs as indicators of this location. However, the apparent spread of the distribution, coupled with relatively high residuals associated with measurements of some of the GerP proteins (stemming from the low brightness of the samples examined), led us to conduct additional measurements with sporulating cells. Brighter fluorescence and improved separation of cells enabled a greater number of individual cells to be included in the analyses, samples for which were drawn from cultures a few hours prior to release of mature spores from mother cells. In this case, the radial locations of all six GerP proteins was more uniform, averaging 445 nm ± 10 nm. The reduced residual values associated with these measurements increase the level of confidence with which we can state that all six GerP proteins reside in a similar location within the inner spore coat. Additionally, none of the GerP-GFP spores cross-reacted with anti-GFP antisera, which is consistent with an inner coat location (data not shown).

GerPA-dependent localization. Having established that the various GerP proteins appear to localize to broadly the same vicinity within the spore, we then sought to identify whether the localization of any individual GerP protein is dependent upon presumed interactions with other protein(s) encoded within the operon. In the first instance, this was achieved by introducing variant pHT315 plasmids containing the *gerP* promoter sequence plus an open reading frame (ORF) encoding the GerP protein of interest with a C-terminal GFP fusion to strains bearing markerless chromosomal deletions in single *gerP* genes. For example, six plasmids encoding GerPA-GFP through GerPF-GFP were introduced individually to the *gerPA* background strain (AG001), and then to the *gerPB* background, and so on, creating a total of 36 new strains. Each of these strains was then sporulated by nutrient exhaustion and analyzed at intervals by fluorescence microscopy until mature spores were released. The results of these analyses reveal that in all backgrounds, with the exception of *gerPA*, the various GerP-GFP fusion proteins are expressed and localize around the developing forespore in a manner reminiscent of that observed for GFP fusion proteins in the wild-type background (Fig. S5). Hence, in the absence of GerPB, for example, all six GFP fusion proteins were observed to localize during sporulation and to persist in the mature spore. The exception to this occurred in the *gerPA* background, where in the absence of GerPA, none of the GerPB-GFP to GerPF-GFP fusion proteins localized around the developing forespore, although diffuse fluorescence interspersed with bright fluorescent foci was observed in the mother cell in each case (Fig. 5). Similar observations were made when the entire *gerP* operon, modified with individual ORFs containing in-frame *gfp* fusions, was expressed in *trans* from a series of plasmids introduced to the *gerP* null

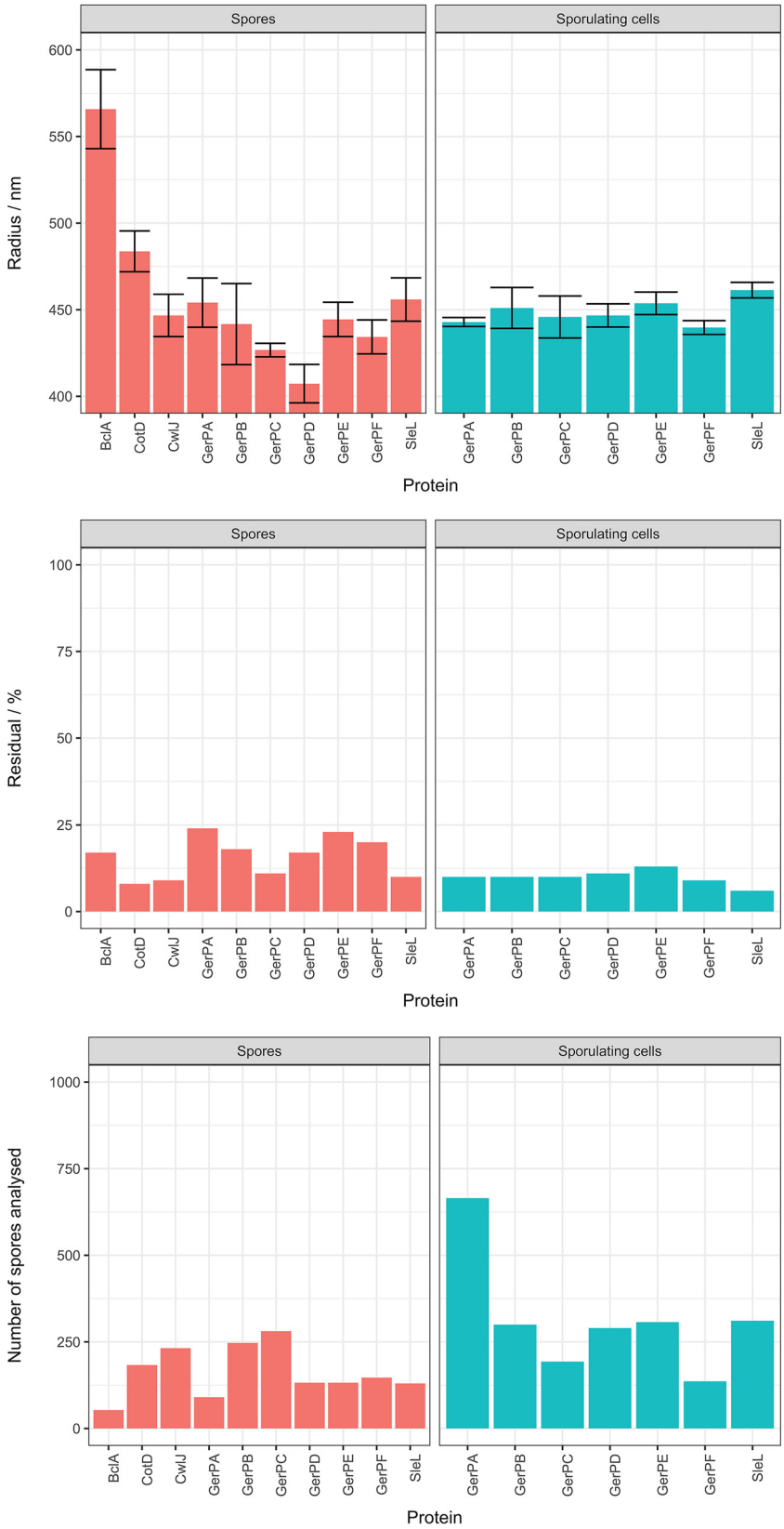

FIG 4 The locations of several GFP-fusion proteins with respect to the spore center were estimated using the ELM image analysis technique. All of the GerP proteins were located near the CLEs SleL and CwlJ, in the inner coat. The number of analyzed spores and the residual error of the model fit are shown and indicate that more accurate estimates were obtained within sporulating cells, just prior to mother cell lysis, than with mature spores, which produced larger residuals attributed to clumping.

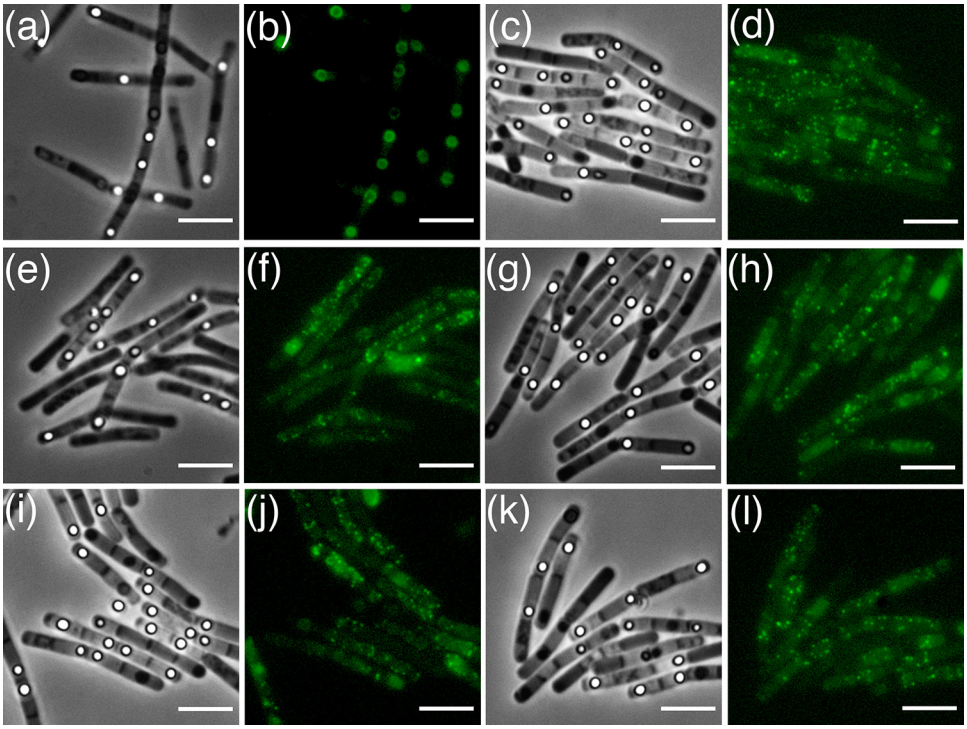

FIG 5 Phase-contrast and fluorescence microscopy of sporulating *B. cereus gerPA* cells with plasmid-borne copies of *gerPA-gfp* (a and b), *gerPB-gfp* (c and d), *gerPC-gfp* (e and f), *gerPD-gfp* (g and h), *gerPE-gfp* (i and j), and *gerPF-gfp* (k and l). None of the remaining GerP proteins can localize around the developing forespore in the absence of GerPA. Scale bar = 5 μm.

background, reducing the potential for differences in expression levels between chromosomal and plasmid-borne genes being responsible for the apparent dependency on GerPA for localization of all other GerP proteins. Similarly, when individual *gerP* genes were introduced on pHT315-derived plasmids to the *gerP* null background, only the GerPA-GFP protein was observed to localize and to produce fluorescent mature spores, conferring further evidence that this protein is key to the localization of the other GerP proteins (Fig. S6).

GerP dependence on coat morphogenetic proteins. A small number of morphogenetic proteins have been identified from genetic and microscopy-based studies that appear to function as interaction hubs for the recruitment and localization of defined subsets of proteins during the assembly of the *B. subtilis* spore coat (13). The SpoIVA protein, for example, is required for the localization of proteins that comprise the basement layer of the coat (15), whereas SafA and CotE are responsible for localizing the inner and outer coat proteins, respectively (16, 17). Although details of the structural hierarchy in terms of morphogenetic protein dependency are sparse in species other than in *B. subtilis*, the conserved presence of genes encoding orthologues of these proteins indicates that SpoIVA, SafA, and CotE probably fulfill related functions in most, if not all, *Bacillus* species (1, 13). With this in mind, and with a view to investigate which, if any, of these proteins are crucial to GerP localization, *spoIVA*, *safA*, and *cotE* null mutant strains were prepared in the *B. cereus* 14579 background. Plasmid-borne copies of *gerPA-gfp* were introduced subsequently to each mutant strain and sporulation allowed to proceed by nutrient starvation. Microscopy analyses revealed that the deletion of *spoIVA* results in early lysis of the developing forespore; hence, this strain was not examined further. In contrast, fluorescence associated with GerPA-GFP was observed in both the *safA* and *cotE* backgrounds (Fig. 6). Localization of the protein, visible as a fluorescent ring encircling the developing forespore, was evident only in the *cotE* background, indicating that GerPA, and presumably by extension all GerP proteins, are SafA-dependent proteins.

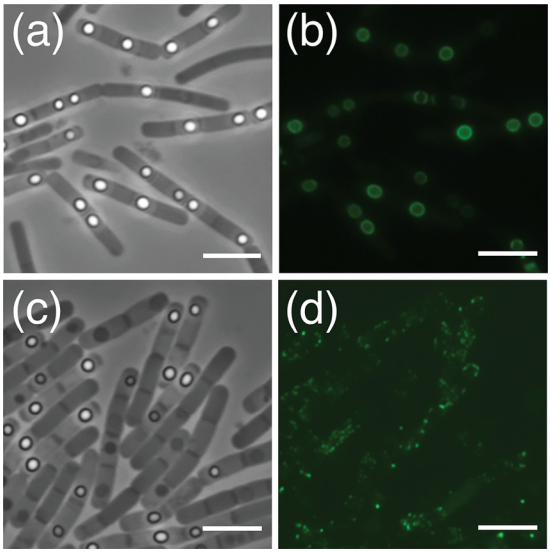

FIG 6 Establishing the localization hierarchy for GerP proteins. Phase-contrast and fluorescence microscopy images of sporulating *B. cereus cotE* cells (a and b) and *safA* cells (c and d), both carrying plasmid-borne *gerPA-gfp* under the control of its native promoter. The GerPA-GFP protein is observed to localize around the developing forespore in the *cotE* background. The same protein is expressed in the *safA* strain but fails to localize, indicating that GerPA, and by extension all GerP proteins, are SafA dependent. These observations are consistent with an inner coat location for the GerP proteins. Scale bar = 5 μm.

Measuring the permeability of GerP spores. The seemingly hindered passage of germinant molecules through the spore coats of various species to interact with the inner membrane-located receptors provides an indirect indication of a permeability defect in *gerP* spores. In an attempt to provide a more direct measurement of the permeability of the coats of wild-type and mutant spores, we examined the possibility of using ELM to measure the diffusion of fluorescein isothiocyanate (FITC)-labeled dextrans of differing sizes through the spore coat. Accordingly, both *B. cereus* and *B. subtilis* wild-type and *gerP* spores were incubated in solutions of FITC-labeled dextrans ranging in size from 3 kDa to 70 kDa, before examination by fluorescence microscopy, as described in Materials and Methods. The best results in terms of amenability to ELM analysis were obtained with *B. subtilis* spores, for which the fluorescence micrographs showed many well-separated spores with bright ring-like images, indicating that an outer portion of the spore had been fluorescently stained (Fig. 7).

Figure 8 presents the midpoint radial locations inferred by ELM analysis for the fluorescent FITC-dextran stains. For every size of FITC-dextran tested, the midpoint of the stained layer was located about 20 nm closer to the spore center in the wild-type spores than in the *gerP* mutants. This is consistent with the notion of impaired coat permeability in the *gerP* mutants that is implied by the germination data; however, the measurement shown in Fig. 8, on its own, would also be consistent with the *gerP* mutants simply being larger than the wild-type spores, so it is essential to consider this result together with the germination data. Additionally, in both the wild type and the *gerP* mutants, the smallest dextran molecules (3 to 5 kDa) were located on average about 15 nm closer to the spore center than the heavier dextrans. The larger dextrans (10, 20, and 70 kDa) were located in similar regions to one another.

DISCUSSION

Bacterial spores of all species are presented with a dilemma in that their protective structures must prevent ingress of potentially damaging molecules or chemicals to the cellular protoplast within while permitting access of small-molecule germinant molecules to the inner membrane-bound germinant receptors. Additionally, they must be capable of rapidly releasing solutes from the spore core, including CaDPA, to the

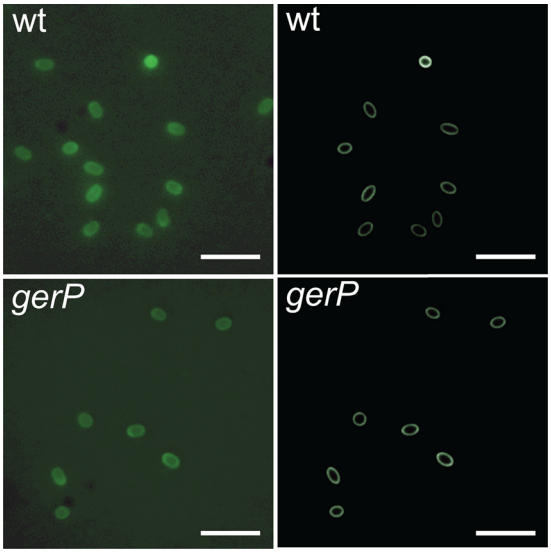

FIG 7 Fluorescence microscopy and superresolved reconstructions of *B. subtilis* wild-type (wt) spores (top panels) and *gerP* spores (bottom panels), stained with FITC-dextrans, with an average molecular mass of 10 kDa. The superresolved reconstructions are generated by feeding precise structure parameters from the fluorescence images back into the ellipsoid model for its image, while decreasing the inferred point spread function to remove instrumental blurring (9). Scale bar = 5 μm.

environment upon spore germination. This is achieved, at least in part, by the presence of a multilayered coat and, in some cases, exosporium structures, one function of which is to serve collectively as molecular sieves (1). The sieving properties vary between species, but in general, it seems that moderately sized proteins and other molecules can breach the outermost layers of spores, exemplified by recent work showing transit of the 26-kDa red fluorescent protein through the exosporium of *Bacillus megaterium* spores and apparently through the outer, but not inner, coat of *B. subtilis* spores (18, 19). These observations are consistent with those of earlier studies (20–22), which imply that permeability decreases with progression toward the interior of the spore.

The results of the germination experiments conducted in this study with *B. cereus* 14579 spores that are null for the entire *gerP* operon, or individual genes therein, are similarly consistent with previous studies and with the hypothesis that the GerP proteins influence the permeability of the spore coat to small hydrophilic molecules. Defective germinative responses were observed, for example, whether induction was via stimulation of the nutrient germinant receptors by alanine or inosine, or in response to exogenous CaDPA or dodecylamine. The result with dodecylamine is in contrast to results observed in *B. subtilis*, where dodecylamine stimulated a faster germinative response in *gerP* spores than in wild-type spores (7). Dodecylamine is known to trigger germination by stimulating the opening of inner membrane-located DPA channels that are present in both *B. subtilis* and *B. cereus* (5); hence, it is not clear why the deletion of *gerP* should cause differing germinative responses between species. The exception to the above-mentioned concerns is *B. cereus gerPF* null spores, which displayed essentially wild-type germinative responses when stimulated via nutrient or nonnutrient pathways. Presumably, the loss of *gerPF* in this case was compensated by either of the two additional *gerPF* homologues encoded elsewhere on the chromosome, as demonstrated previously in closely related *B. anthracis* spores (8).

A primary objective of this study was to ascertain whether the GerP proteins are structural components of the spore or whether they are involved only in spore assembly. Fluorescence microscopy of strains expressing GerP-GFP fusion proteins supports the notion that GerP proteins are indeed located in the spore coat, and the images of smooth fluorescent rings appeared suitable for ELM image analysis using a spherical shell model as an approximation to the GerP-GFP location. We then used ELM

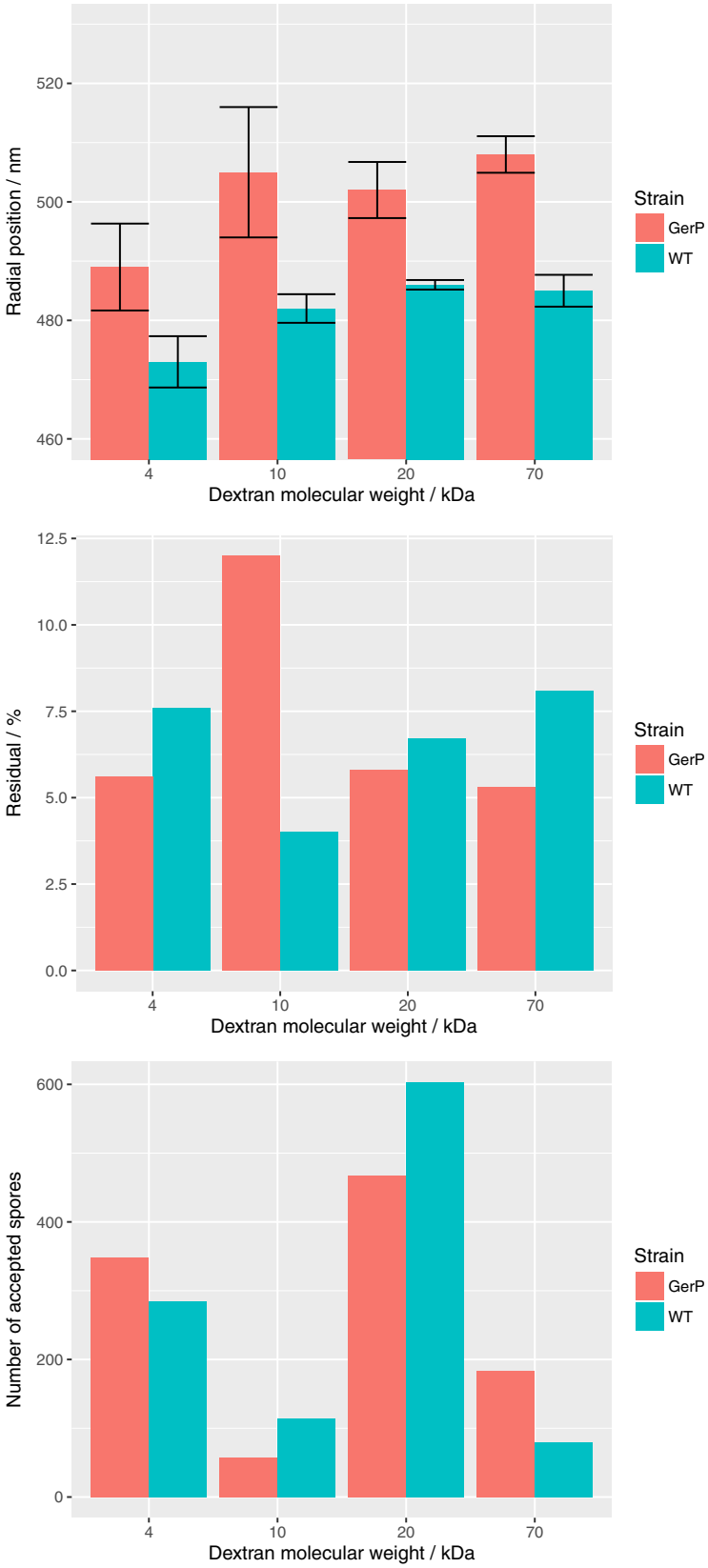

FIG 8 The midpoint radial locations of regions of *B. subtilis* spores fluorescently stained with FITC-dextran molecules were inferred using the ELM image analysis technique. The number of analyzed spores and average residual error of the model fits are also shown for each case.

to more precisely locate the GerP proteins with respect to some other coat and exosporium proteins. These included the BclA exosporial nap protein, coat-localized CotD, and the CLEs CwlJ and SleL. The radial location of each of these benchmark proteins was established using ELM; BclA, as expected, was outermost, followed by CotD, and then SleL and CwlJ. The SleL and CwlJ proteins occupied a similar radial location around 450 nm, which we identify as the position of the inner coat. Overall, we found that all the GerP proteins were also located in the inner coat. Our analysis of GerP locations in mature spores was, unfortunately, complicated by the fact that the spores tended to clump, and hence, the number of well-separated spores available for analysis was limited. Additionally, even the available images were often poorly fitted due to adjacent fluorescent material. The high residual fitting errors shown in Fig. 4 indicate that the radial locations found for the GerP proteins in mature spores (407 to 454 nm) have limited accuracy and may be biased by image analysis limitations. In order to obtain more accurate estimates of GerP location, additional fluorescence microscopy was conducted with sporulating GerP-GFP cells in which the fluorescent proteins were observed to have completely localized to rings around phase-bright forespores but prior to mother cell lysis. We obtained superior fluorescence brightness with these samples, and much more importantly, we found that this removed many of the difficulties due to spore clumping and enabled a greater number of cells to be analyzed. Subject to the assumption that the GerP protein locations in these specimens are consistent with their locations in mature spores, we believe this method more accurately located the GerP proteins. These results, in which the GerP protein radial locations span a narrower range from 440 nm to 454 nm, indicate that all six proteins remain in the inner coat but now seem more likely to share proximity with CwlJ (447 nm) and SleL (456 nm) within the spore (SleL was also observed to occupy a similar location in both sporulating cells and in mature spores). This is an important distinction, since the location of CLEs in the inner spore coat could pose a mechanistic problem as to how they access the cortical substrate during germination, especially if the GerP proteins form a proteinaceous layer that lies between the CLEs and the cortex/outer membrane boundary. A future objective will be to improve the resolution of these measurements to definitively ascertain the location of CLEs with respect to the cortex.

A further objective of this work was to establish the localization hierarchy for the GerP proteins, both in terms of morphogenetic protein dependency and to identify any dependency between the individual GerP proteins. With regard to morphogenetic protein dependency, fluorescence microscopy analyses conducted with *B. cereus cotE* and *safA* spores revealed GerPA, and therefore presumably all GerP proteins, to be SafA dependent. Hence, the SafA protein's role as the interaction hub for inner coat localization in *B. subtilis* spores appears to be conserved in *B. cereus* spores, and again, presumably across all *Bacillus* species. Similar fluorescence microscopy-based analyses conducted with a series of null mutants and appropriate GerP-GFP-expressing strains indicate that only the GerPA protein is required for each of the remaining GerP proteins to localize in the developing spore. We cannot rule out, however, that one or both of the additional GerPF homologues encoded on the chromosome permit localization of GerPA-GerPE in the *gerPF* null mutant; this is something that will have to be tested in the future. Regardless, we can infer from these analyses that the GerPB, GerPC, GerPD, and GerPE proteins each have an essential role in maintaining the permeability of the coat to permit ingress of germinants to their sites of interaction with receptors at the inner membrane. GerPA is also essential, although whether this goes beyond its requirement for localization of the remaining GerP proteins or whether it has an additional function relating to spore permeability has yet to be established. Unfortunately, preliminary experiments aimed at identifying physical interactions that may occur between the GerP proteins using a bacterial 2-hybrid system were unsuccessful, owing in part to the relative insolubility of at least some of the proteins when expressed in *Escherichia coli* (data not shown).

Finally, the ELM technique was applied to compare the permeabilities of wild-type and *gerP* spores, since it offered the prospect of making direct quantitative measure-

ments using fluorescent dextran stains as opposed to inferring permeability defects based on germination kinetics. Measurements with wild-type *B. subtilis* spores revealed that the smallest FITC-dextran tested (3 to 5 kDa) permeated to a depth that is comparable in location to the CotG protein when measured by the same method (radial locations of 473 nm versus 475 nm [9]), whereas the larger dextrans localized to a position comparable to the location of the CotZ outer crust protein (485 nm versus 480 nm [9]). In contrast, midpoint radial locations for all dextran-stained *gerP* spores measured outside the location of the wild-type CotZ protein (489 nm for 3- to 5-kDa dextrans and ~505 nm for the larger dextrans). Since CotZ is located on the surface of *B. subtilis* spores (3), these data indicate that none of the dextran stains significantly permeated the *gerP* spores, instead adhering and accumulating on the spore surface. This may be too simplistic a view, however, since the layer order of proteins in wild-type spores may not apply to *gerP* spores, and indeed, a previous study includes a transmission electron microscopy (TEM) image of a single *B. subtilis gerP* spore that appears to lack the spore crust (23). It is intriguing, therefore, that despite being located in the inner coat, the GerP proteins appear to exert an influence on the permeability of the coat that extends to the surface of the spore. One possible explanation for this is that absence of GerP proteins in the inner coat results in relatively subtle structural perturbations that ripple through to the layers on top, perhaps even leading to loss of the crust. This hypothesis will be tested in future by establishing the layer order and precise locations of defined coat proteins in *gerP* spores with respect to those in wild-type spores.

MATERIALS AND METHODS

Bacterial strains and spore preparation. The *Bacillus cereus* strains employed in this study (Table 1) were all isogenic with the ATCC 14579 strain, which was a gift from Toril Lindbäck (Norwegian School of Veterinary Science, Norway). *Bacillus cereus* strains were routinely cultured in LB medium at 30°C, supplemented with 1 μg/ml erythromycin and 25 μg/ml lincomycin where appropriate (Table 1). Competent *Escherichia coli* DH5α cells (NEB UK) were used for cloning procedures and for the propagation of plasmids. *Bacillus cereus* spores were prepared by nutrient exhaustion in casein-hydrolysate yeast-extract (CCY) liquid medium (24). Efficient sporulation was achieved using 200-ml cultures in 2-liter baffled flasks that were subject to orbital agitation at 30°C for 48 h. The resultant spores were purified from cellular debris by centrifuging and resuspending the spore pellets initially in phosphate-buffered saline (PBS) supplemented with 0.1% (wt/vol) Tween 20, followed by several rounds of washing and resuspending spores in ice-cold deionized water. Spores of *B. subtilis* strains were prepared by sporulation at 37°C on 2× Schaeffer's glucose agar plates without antibiotics, as described previously (7). Purified spores of both species were stored as suspensions (optical density at 600 nm [OD_{600}], 50) in water at 4°C.

Mutant construction. A series of *gerP* null mutant strains in the *B. cereus* 14579 background were constructed using a markerless allelic exchange methodology (19, 25). To delete *gerPA* (BC1145), for example, PCR was used to prepare an amplicon comprising approximately 500 bp of sequence upstream and inclusive of the *gerPA* start codon. A second amplicon comprising 500 bp of downstream sequence starting from, and including the *gerPA* stop codon, was also prepared by PCR. Primers were designed to include approximately 15 bp of overlapping sequence between the 3′ end of the upstream amplicon and the 5′ end of the downstream amplicon (sequences of primers used in this work are shown in Tables 2 to 5). Additionally, the 5′ end of the upstream amplicon contained 15 bp of overlapping sequence with the 5′ end of EcoRI- and BamHI-digested pMAD vector (26), as did the 3′ end of the downstream amplicon with the 3′ end of pMAD. A variant pMAD vector containing a single I-SceI restriction site was used in this work (a gift from Toril Lindbäck, Norwegian School of Veterinary Science, Oslo, Norway). The fragments were assembled using a Klenow-based ligation independent cloning technique (https://openwetware.org/wiki/Klenow_Assembly_Method:_Seamless_cloning) and then used to transform *E. coli* to carbenicillin resistance. Transformant *E. coli* strains were screened by colony PCR to identify clones with the correct construct, and plasmids were subsequently purified and validated by DNA sequencing. Similar procedures were used to prepare plasmids designed to individually delete the remaining *gerP* genes (*gerPB* [BC1144], *gerPC* [BC1143], *gerPD* [BC1142], *gerPE* [BC1141], and *gerPF* [BC1140]) and to delete the entire operon.

pMAD-derived plasmids were subsequently introduced to *B. cereus* by electroporation, with transformants being selected at 30°C on LB plates supplemented with 1 μg/ml erythromycin, 5 μg/ml lincomycin, and 90 μg/ml 5-bromo-4-chloro-3-indolyl-β-D-galactopyranoside (X-Gal). Electroporation was conducted using a Gene Pulsar instrument (Bio-Rad), operating at 200 Ω, 2 kV, and 25 μF, and cuvettes that contained 500 ng of plasmid DNA plus 50 μl of thawed electrocompetent cells. Clones that had integrated plasmids by homologous recombination were selected by incubating blue colonies at 37°C on fresh LB plates and restreaking after 24 and 48 h. Plasmid pBKJ223, which encodes the I-SceI restriction enzyme, was introduced by electroporation to single-crossover cells, which were recovered on LB

TABLE 2 Oligonucleotide primers used to create null mutant strains

Strain mutant type	Primer	Sequence (5′ to 3′)
gerPA	pMAD *gerPA* up For	CCATGGTACCCGGGAGCTCGAATTCCTCATACCCTTTAATTGTATTCGCA
	ATGTAA *gerPA* up Rev	AAAAATTCAATGCAATTGCCTCCTTTACATACAAAACACCCTTCGTTTTT
	ATGTAA *gerPA* down For	AAAAACGAAGGGTGTTTTGTATGTAAAGGAGGCAATTGCATTGAATTTTT
	pMAD *gerPA* down Rev	GCCTCGCGTCGGGCGATATCGGATCCAAACCAATATTTAAAGTACCATTT
gerPB	pMAD *gerPB* up For	GCCATGGTACCCGGGAGCTCGAATTCGCGATTGAAAAAAAACGTGAAAAA
	ATGTAA *gerPB* up Rev	ATATTTATGACAAGGATGTCTTACATTGCAATTGCCTCCTTTAAGTTGAG
	ATGTAA *gerPB* down For	GCTCAACTTAAAGGAGGCAATTGCAATGTAAGACATCCTTGTCATAAATA
	pMAD *gerPB* down Rev	GCCTCGCGTCGGGCGATATCGGATCCCATCCACCATCATTTGTCGATACA
gerPC	pMAD *gerPC* up For	GCATGCCATGGTACCCGGGAGCTCGAATTCTGGTCGGACATATTCGTATC
	ATGTAA *gerPC* up Rev	CGTTAAGGTTCATACATACTTACATTTGTGAAACCTCCTTTTCAATAGGG
	ATGTAA *gerPC* down For	CCCTATTGAAAAGGAGGTTTCACAAATGTAAGTATGTATGAACCTTAACG
	pMAD *gerPC* down Rev	GCCTCGCGTCGGGCGATATCGGATCCAAAAGTGTGCGCAATTCAACGTTA
gerPD	pMAD *gerPD* up For	GCATGCCATGGTACCCGGGAGCTCGAATTCAAAATCGCCCCTCCTCTTCT
	ATGTAA *gerPD* up Rev	ATAATTTTTCAGTCTCCTTACATACATACTTACTCCTTTCGGAAATTTC
	ATGTAA *gerPD* down For	GAAATTTCCGAAAGGAGTAAGTATGTATGTAAGGAGACTGAAAAATTAT
	pMAD *gerPD* down Rev	CCTCGCGTCGGGCGATATCGGATCCAATTGAAAGAACCGTTACTGTTTTG
gerPE	pMAD *gerPE* up For	TGCATGCCATGGTACCCGGGAGCTCGAATTCAAAATCGCCCCTCCTCTTC
	ATGTAA *gerPE* up Rev	CATAATTTTTCAGTCTCCTTACATACATACTTACTCCTTTCGGAAATTTC
	ATGTAA *gerPE* down For	GAAATTTCCGAAAGGAGTAAGTATGTATGTAAGGAGACTGAAAAATTATG
	pMAD *gerPE* down Rev	GCCTCGCGTCGGGCGATATCGGATCCAATTGAAAGAACCGTTACTGTTTTG
gerPF	pMAD *gerPF* up For	TGCATGCCATGGTACCCGGGAGCTCGAATTCAACAGTTACAGAGGGTCCA
	ATGTAA *gerPF* up Rev	AGAATATCTCCTACTTTTTTTACATCCACCTACTTTACTAAACTTTGTAA
	ATGTAA *gerPF* down For	TTACAAAGTTTAGTAAAGTAGGTGGATGTAAAAAAAGTAGGAGATATTCT
	pMAD *gerPF* down Rev	CCTCGCGTCGGGCGATATCGGATCCAACATCCTGTAAAAGAGAAATGTTT
gerP (operon)	pMAD *gerP* up For	GCCATGGTACCCGGGAGCTCGAATTCTCTCCATCCTAAAACT
	ATGTAA *gerP* up Rev	CTTGTTTATACCACTATTACATTTATTGCGTGTGTGTTTTGAACG
	ATGTAA *gerP* down For	CGTTCAAAACACACACGCAATAAATGTAATAGTGGTATAAACAAGTAAG
	pMAD *gerP* down Rev	GCCTCGCGTCGGGCGATATCGGATCCAGAAAAGCTTACAACATCCTGT
cotE	pMAD *cotE* up For	CCATGGTACCCGGGAGCTCGAATTCATTTCTGAAACAGAAGAAGTTGATT
	ATGTAA *cotE* up Rev	ACTTCTCCCTAGCTTTCTATTACATTCGTAACCCTCCTCAATCACTATTC
	ATGTAA *cotE* down For	TAGAAAGCTAGGGAGAAGTTCTTCC
	pMAD *cotE* down Rev	CCTCGCGTCGGGCGATATCGGATCCAATTGTACTACTTCACGACGTACTA
safA	pMAD *safA* up For	CCATGGTACCCGGGAGCTCGAATTCATATGATTGAATCAGCGCCACCTGG
	ATGTAA *safA* up Rev	CGGGAATACTCCCGCCTTTTTACATATTTTCCCCCTCCTGTATAACTTAT
	ATGTAA *safA* down For	AAATATGTAAAAAGGCGGGAGTATTCCCGCCTTTT
	pMAD *safA* down Rev	CCTCGCGTCGGGCGATATCGGATCCCTGTTTTACCATCATTGTTAATGTA

medium containing 10 μg/ml tetracycline. Transformant colonies were subsequently passaged every 24 h in fresh LB medium containing tetracycline at 37°C, with aliquots being plated and screened on LB agar containing tetracycline and X-Gal for white colonies that were sensitive to erythromycin and lincomycin. Candidate colonies that had undergone a second recombination event to excise the integrated plasmid, leaving behind the truncated gene, were validated by PCR and sequencing and then passaged on LB medium minus antibiotics to promote excision of the pBKJ223 plasmid. The same markerless deletion strategy was used to create *B. cereus* 14579-derived strains that were null for the coat morphogenetic proteins SpoIVA (BC1509), SafA (BC4420), and CotE (BC3770).

The low-copy-number episomal plasmid pHT315 (27) was used as the basis to construct a series of GerP-GFP fusion strains. Two different strategies were employed. First, overlap PCR was used to construct

TABLE 3 Oligonucleotide primers used to validate null mutant strains by diagnostic PCR

Strain mutant type	Primer	Sequence (5′ to 3′)
gerPA	*gerPA* Out For	GTCATGTACATACGGATTTACACCCTAATCAAACGTTCAAAACACACACG
	gerPA Out Rev	GATAGGGCTTTAATACTTCCGGCAGTACCAATTTGGAACACAGAAGAGG
gerPB	*gerPB* Out For	CCGGCTCTTTCAACGTTGGAGATAATGTTTCTGTCTACAATTATCA
	gerPB Out Rev	GCTCTTCTTGGAGTTGGCGCACTTGATCTTCTAAATTTAGGATGGCTGC
gerPC	*gerPC* Out For	GGTACTGCCGGAAGTATTAAAGCCCTATCTAAATTTTCAAATACGGGCGG
	gerPC Out Rev	CGGACGACGATACACCGTTCATTTTAATCTGTCCGACTTTTAACTCACGG
gerPD	*gerPD* Out For	GCATCGACTCCCTTATTATTTATCACAAGCGCAATCATATGAAGGTA
	gerPD Out Rev	CTCCCCGTATATAACAAGGAATTTCACGGTGGACGGCAATAGCTCTAC
gerPE	*gerPE* Out For	GCCTTTCTCTCCTTTATTCAGCACATACCGGGAAATTTCCGAAAGGAG
	gerPE Out Rev	GATCTGCCACATCAGAATCAAATGTATTCGTTGCACTAACACCGTTAAAC
gerPF	*gerPF* Out For	GCGCACACTTTTAAACTCTGGTGGATTTCAAATTGGAAATGTTGATTATG
	gerPF Out Rev	TAGTGCCTCTTCACTACTTACTTGTTTATACCACTATTTGTGGAC
gerP	*gerP* Out For	CGGCGCTAATATTTTCACCTCTGTTAACGGATAATACGCCGCTTCCCCG
	gerP Out Rev	GATGCTTGCAGCAGAAGAAGCATATCAAGATTGGCAAGGGAAGAGTG

TABLE 4 Oligonucleotide primers used to create GFP fusion strains

Primer	Sequence (5′ to 3′)	Overlap
gfp For	AGTAAAGGAGAAGAACTTTTCACTGGAGTTGTCCCAATTCTTGTTGAATT	
gfp Rev	TTATTTGTATAGTTCATCCATGCCATGTGTAATCCCAGCAGCTGTTACAA	
pHT315 Prom *gerPA* For	CAGCTATGACCATGATTACGCCAAGCTTTCATTTGGCATAAAATGTAG	pHT315
pHT315 *gerPF* Rev	GTTGTAAAACGACGGCCAGTGAATTCTTACGCTGTTCCAATCTGATCTTG	pHT315
gfp gerPA Rev	CCAGTGAAAAGTTCTTCTCCTTTACTAGTTGAGCCAATTATCGCTTGATC	*gfp*
gfp gerPB For	GCATGGATGAACTATACAAATAAAGGAGGCAATTGCATTGAATTTTTA	*gfp*
gfp gerPB Rev	GTGAAAAGTTCTTCTCCTTTACTAGAAGAACTAGTTGATGGTTTGATAG	*gfp*
gfp gerPC For	GGCATGGATGAACTATACAAATAAGACATCCTTGTCATAAATATATAGCA	*gfp*
gfp gerPC Rev	CCAGTGAAAAGTTCTTCTCCTTTACTCTCCTTTCGGAAATTTCCCGGTAT	*gfp*
gfp gerPD For	GGCATGGATGAACTATACAAATAAGTATGTATGAACCTTAACGTTGTAAA	*gfp*
gfp gerPD Rev	CTCCAGTGAAAAGTTCTTCTCCTTTACTACCTGGAGTAGGAGGGACATCT	*gfp*
gfp gerPE For	GGCATGGATGAACTATACAAATAAGGAGACTGAAAAATTATGTTGCATCA	*gfp*
gfp gerPE Rev	CCAGTGAAAAGTTCTTCTCCTTTACTTTGTGCGGAAGGTTCATCTGTAAT	*gfp*
gfp gerPF For	CATGGCATGGATGAACTATACAAATAATTCATATAGTAATTACAAAGTTT	*gfp*
gfp gerPF Rev	GTGAAAAGTTCTTCTCCTTTACTCGCTGTTCCAATCTGATCTTGATCTG	*gfp*
pHT315 *gfp* Rev	GTTGTAAAACGACGGCCAGTGAATTCTTATTTGTATAGTTCATCCATGCC	*gfp*

six variant *gerP* operons, each of which contained the native promoter sequence followed by *gerPA* through *gerPF*. In each variant plasmid, a single *gerP* gene, minus the stop codon, was fused at the 3′ end with an amplicon encoding the gene for GFP. Fragments containing the *gerP* promoter sequence, variant *gerP* operons, and linearized pHT315 were assembled using the Klenow assembly technique and used to transform *E. coli* to carbenicillin resistance. A similar approach was used to construct pHT315-derived plasmids containing the *gerP* promoter sequence and single *gerP* genes fused at the 3′ end with *gfp*. Constructs containing *gfp* fusions to *bclA* (BC1207), *cotD* (BC1560), *sleL* (BC3607), and *cwlJ* (BC5390), each under the control of their native promoter sequences, were prepared similarly. In all cases, the resultant plasmids were purified from positive *E. coli* clones, validated for the intended construction by DNA sequencing, and introduced to *B. cereus* wild-type and *gerP* null strains by electroporation.

Spore germination assays. Spore germination assays were conducted using spores that were synchronized to germinate by incubating at 70°C for 15 min and then cooling on ice. Spores (300 μl) were resuspended at an optical density at 600 nm (OD_{600}) of 1 (approximately 10^8 spores · ml^{-1}) in 10 mM Tris-HCl buffer (pH 7.4), supplemented with 10 to 100 mM L-alanine or inosine, and the resultant changes in absorbance were monitored at 30°C using a PerkinElmer EnVision Xcite multilabel plate reader fitted with a 600-nm photometric filter. Germination experiments conducted with nonphysiological germinants were conducted by resuspending spores at an OD_{600} of 1 in 2.5 mM Tris-HCl (pH 7.4) supplemented with 50 mM CaDPA at 30°C, or in 25 mM KPO_4 (pH 7.5), supplemented with 1 mM dodecylamine at 45°C. Changes in absorbance of the spore suspensions were monitored as described above. The presented data are from single experiments, which are representative of multiple analyses conducted with at least two batches of spores. Spore viability was assessed by plating serially diluted spore suspensions on LB agar plates, followed by colony enumeration after 24 h of incubation at 30°C.

Microscopy. Three microliters of spore or cellular suspensions was dispersed onto poly-L-lysine-coated microscope slides and sealed under a coverslip. The samples were imaged on an Olympus BX53 microscope with a 100× 1.30 numerical aperture (NA) oil objective lens, illumination from a mercury lamp, and filters for GFP and red fluorescence (i.e., FM4-64 dye was added to some samples to enable visualization of membranes). Images were captured with a Retiga-2000R charge-coupled-device (CCD)

TABLE 5 Oligonucleotide primers used to create *gfp* fusions to defined spore coat proteins

Strain genotype	Primer	Sequence (5′ to 3′)
bclA-gfp	pHT315 *bclA* For	GCTATGACCATGATTACGCCAAGCTTCTTCCAAATCAATCATATGTTATA
	bclA gfp Rev	CAGTGAAAAGTTCTTCTCCTTTACTAGCGATTTTTTCAATAATAATAGAT
	bclA gfp For	ATCTATTATTATTGAAAAAATCGCTAGTAAAGGAGAAGAACTTTTCACTG
	pHT315 *gfp* Rev	GTTGTAAAACGACGGCCAGTGAATTCTTATTTGTATAGTTCATCCATGCC
cotD-gfp	pHT315 *cotD* For	GCTATGACCATGATTACGCCAAGCTTTGCCACCACCATCTCCGTATGC
	cotD gfp Rev	CCAGTGAAAAGTTCTTCTCCTTTACTCTTTTTAAATATTCCACCAACG
	cotD gfp For	CGTTGGTGGAATATTTAAAAAGAGTAAAGGAGAAGAACTTTTCACTGG
sleL-gfp	pHT315 *sleL* For	CTATGACCATGATTACGCCAAGCTTCATACCACTCAGGATATAACTTTTT
	sleL gfp Rev	CAGTGAAAAGTTCTTCTCCTTTACTGCCCTTTTTCGTAATCGTAAAGTTT
	sleL gfp For	AAACTTTACGATTACGAAAAAGGGCAGTAAAGGAGAAGAACTTTTCACTG
cwlJ-gfp	pHT315 *cwlJ* For	GCTATGACCATGATTACGCCAAGCTTAGATACCAAAGTAGGCTCAATTAC
	gfp cwlJ Down	CCAGTGAAAAGTTCTTCTCCTTTACTATATACGCTAGGGCAGTCTTCGCC
	cwlJ gfp Up	GGCGAAGACTGCCCTAGCGTATATAGTAAAGGAGAAGAACTTTTCACTGG
	cwlJ gfp Down	TCCCTCCTCATTTTCATCTCTTATTTGTATAGTTCATCCATGCC
	gfp gerQ Up	GGCATGGATGAACTATACAAATAAGAGATGAAAATGAGGAGGGA
	pHT315 *gerQ* down	CGACGTTGTAAAACGACGGCCAGTGAATTCTTATGGTCTTGGAGTATAAG

camera, giving a pixel width of 74 nm on the specimen, and 12-bit gray levels. The image data were recorded as 1,600 by 1,200 pixel Tiffs.

Immunolabeling of spores. Spores (1 ml; OD_{600}, 10) were incubated with gentle agitation at room temperature in phosphate-buffered saline (PBS) containing 2% (wt/vol) bovine serum albumin (BSA) for 1 h. Spores were harvested by centrifugation (13,500 × *g* for 1 min), resuspended in 400 μl PBS-BSA, and incubated with 100 μl of 500-fold diluted anti-GFP antibody (ab290; Abcam, Cambridge, UK) for 30 min, followed by three washes in PBS-BSA. Resuspended spores (400 μl) were then incubated with 100 μl of 500-fold diluted Dylight594-conjugated anti-rabbit IgG antibody (ab96885; Abcam) for 30 min. Antibody-labeled spores were washed three times with PBS-BSA and then analyzed by fluorescence microscopy.

Dextran permeability experiments. A series of fluorescein isothiocyanate (FITC)-labeled dextrans (Sigma-Aldrich, Dorset, UK), with average molecular masses of 3 to 5 kDa, 10 kDa, 20 kDa, and 70 kDa, were used to investigate the permeabilities of *B. subtilis* wild-type and *gerP* spores. Essentially, 50 μl of the respective FITC-dextran solutions (25 mg/ml) were added to the same volume of spores (OD_{600}, 10), which were then incubated for 24 h at 4°C. In order to reduce background fluorescence, the dextran-spore suspensions were pelleted by centrifugation (13,500 × *g* for 1 min), enabling removal of the unbound dextran-containing supernatant, before resuspending the spores in 1 ml of sterile deionized (DI) water. The spores were centrifuged again and resuspended in 100 μl of water, and then 3 μl of the suspension were transferred to poly-L-lysine-coated microscope slides for imaging by fluorescence microscopy.

Ellipsoid localization microscopy. The quantitative fluorescence ELM technique was used to measure the location of GFP fusion proteins in mature spores and in sporulating cells, as well as to measure the extent to which fluorescently labeled dextran molecules had permeated spores. The ELM analysis was previously reported in detail (9). Briefly, several independent fields of GFP- or FITC-dextran-labeled spores or sporulating cells were imaged with fluorescence microscopy. Each field contained about 50 spores or cells on a dark background. Automated image segmentation was used to identify single spores, and the image of each candidate was used to fit the parameters of a model that describes the image of a spheroidal fluorescent shell. For *B. cereus*, an equation describing the image of a spherical fluorescent layer was fitted to the image data; for *B. subtilis*, a model for an ellipsoidal shell was fitted because this spore cannot be well approximated by a sphere. A filter was applied to exclude fits from overlapping spores and fragments of debris. The average radius parameter fitted to the spores provides an estimate of the midpoint radial position of the GFP fusion or FITC-dextran layer with respect to the spore center. (The equivalent radius of a sphere of equal volume is reported for FITC-dextran layers that were analyzed with the ellipsoid model.) The mean and standard deviation of the estimates from several fields of spores or cells with each protein are presented in Fig. 4 and 8. Sample data and ELM software are provided in supporting data (https://doi.org/10.17863/CAM.23124).

SUPPLEMENTAL MATERIAL

Supplemental material for this article may be found at https://doi.org/10.1128/AEM.00760-18.

SUPPLEMENTAL FILE 1, PDF file, 3.0 MB.

ACKNOWLEDGMENTS

We declare no competing financial interests.

A.G. was the recipient of a Cambridge Nehru Scholarship and received support from the Raymond and Beverly Sackler Foundation. We gratefully acknowledge support from MedImmune through the Beacon collaboration, and from the Engineering and Physical Sciences Research Council Centre for Doctoral Training in Sensor Technologies and Applications (grant EP/L015889/1).

REFERENCES

1. Henriques AO, Moran CP, Jr. 2007. Structure, assembly, and function of the spore surface layers. Annu Rev Microbiol 61:555–588. https://doi.org/10.1146/annurev.micro.61.080706.093224.
2. Stewart GC. 2015. The exosporium layer of bacterial spores: a connection to the environment and the infected host. Microbiol Mol Biol Rev 79:437–457. https://doi.org/10.1128/MMBR.00050-15.
3. McKenney PT, Driks A, Eichenberger P. 2013. The *Bacillus subtilis* endospore: assembly and functions of the multilayered coat. Nat Rev Microbiol 11:33–44. https://doi.org/10.1038/nrmicro2921.
4. Popham DL, Bernhards CB. 2015. Spore peptidoglycan. Microbiol Spectr 3:157–177. https://doi.org/10.1128/microbiolspec.TBS-0005-2012.
5. Setlow P. 2014. Germination of spores of *Bacillus* species: what we know and do not know. J Bacteriol 196:1297–1305. https://doi.org/10.1128/JB.01455-13.
6. Behravan J, Chirakkal H, Masson A, Moir A. 2000. Mutations in the *gerP* locus of *Bacillus subtilis* and *Bacillus cereus* affect access of germinants to their targets in spores. J Bacteriol 182:1987–1994. https://doi.org/10.1128/JB.182.7.1987-1994.2000.
7. Butzin XY, Troiano AJ, Coleman WH, Griffiths KK, Doona CJ, Feeherry FE, Wang G, Li YQ, Setlow P. 2012. Analysis of the effects of a *gerP* mutation on the germination of spores of *Bacillus subtilis*. J Bacteriol 194:5749–5758. https://doi.org/10.1128/JB.01276-12.
8. Carr KA, Janes BK, Hanna PC. 2010. Role of the *gerP* operon in germination and outgrowth of *Bacillus anthracis* spores. PLoS One 5:e9128. https://doi.org/10.1371/journal.pone.0009128.
9. Manetsberger J, Manton JD, Erdelyi MJ, Lin H, Rees D, Christie G, Rees EJ. 2015. Ellipsoid localization microscopy infers the size and order of protein layers in *Bacillus* spore coats. Biophys J 109:2058–2066. https://doi.org/10.1016/j.bpj.2015.09.023.
10. Sylvestre P, Couture-Tosi E, Mock M. 2002. A collagen-like surface gly-

coprotein is a structural component of the *Bacillus anthracis* exosporium. Mol Microbiol 45:169–178. https://doi.org/10.1046/j.1365-2958.2000.03000.x.
11. Todd S, Moir A, Johnson M, Moir A. 2003. Genes of *Bacillus cereus* and *Bacillus anthracis* encoding proteins of the exosporium. J Bacteriol 185:3373–3378. https://doi.org/10.1128/JB.185.11.3373-3378.2003.
12. Eijlander RT, Kuipers OP. 2013. Live-cell imaging tool optimization to study gene expression levels and dynamics in single cells of *Bacillus cereus*. Appl Environ Microbiol 79:5643–5651. https://doi.org/10.1128/AEM.01347-13.
13. Driks A, Eichenberger P. 2016. The spore coat. Microbiol Spectr 4:179–200. https://doi.org/10.1128/microbiolspec.TBS-0023-2016.
14. Steichen CT, Kearney JF, Turnbough CL, Jr. 2005. Characterization of the exosporium basal layer protein BxpB of *Bacillus anthracis*. J Bacteriol 187:5868–5876. https://doi.org/10.1128/JB.187.17.5868-5876.2005.
15. Ramamurthi KS, Losick R. 2008. ATP-driven self-assembly of a morphogenetic protein in *Bacillus subtilis*. Mol Cell 31:406–414. https://doi.org/10.1016/j.molcel.2008.05.030.
16. Little S, Driks A. 2001. Functional analysis of the *Bacillus subtilis* morphogenetic spore coat protein CotE. Mol Microbiol 42:1107–1120. https://doi.org/10.1046/j.1365-2958.2001.02708.x.
17. Ozin AJ, Henriques AO, Yi H, Moran CP, Jr. 2000. Morphogenetic proteins SpoVID and SafA form a complex during assembly of the *Bacillus subtilis* spore coat. J Bacteriol 182:1828–1833. https://doi.org/10.1128/JB.182.7.1828-1833.2000.
18. Donadio G, Lanzilli M, Sirec T, Ricca E, Isticato R. 2016. Localization of a red fluorescence protein adsorbed on wild type and mutant spores of *Bacillus subtilis*. Microb Cell Fact 15:153. https://doi.org/10.1186/s12934-016-0551-2.
19. Lindbäck T, Mols M, Basset C, Granum PE, Kuipers OP, Kovacs AT. 2012. CodY, a pleiotropic regulator, influences multicellular behaviour and efficient production of virulence factors in *Bacillus cereus*. Environ Microbiol 14:2233–2246. https://doi.org/10.1111/j.1462-2920.2012.02766.x.
20. Gerhardt P, Black SH. 1961. Permeability of bacterial spores. II. Molecular variables affecting solute permeation. J Bacteriol 82:750–760.
21. Koshikawa T, Beaman TC, Pankratz HS, Nakashio S, Corner TR, Gerhardt P. 1984. Resistance, germination, and permeability correlates of *Bacillus megaterium* spores successively divested of integument layers. J Bacteriol 159:624–632.
22. Nishihara T, Takubo Y, Kawamata E, Koshikawa T, Ogaki J, Kondo M. 1989. Role of outer coat in resistance of *Bacillus megaterium* spore. J Biochem 106:270–273. https://doi.org/10.1093/oxfordjournals.jbchem.a122843.
23. Nagler K, Setlow P, Reineke K, Driks A, Moeller R. 2015. Involvement of coat proteins in *Bacillus subtilis* spore germination in high-salinity environments. Appl Environ Microbiol 81:6725–6735. https://doi.org/10.1128/AEM.01817-15.
24. Xu Zhou K, Wisnivesky F, Wilson DI, Christie G. 2017. Effects of culture conditions on the size, morphology and wet density of spores of *Bacillus cereus* 569 and *Bacillus megaterium* QM B1551. Lett Appl Microbiol 65:50–56. https://doi.org/10.1111/lam.12745.
25. Janes BK, Stibitz S. 2006. Routine markerless gene replacement in *Bacillus anthracis*. Infect Immun 74:1949–1953. https://doi.org/10.1128/IAI.74.3.1949-1953.2006.
26. Arnaud M, Chastanet A, Debarbouille M. 2004. New vector for efficient allelic replacement in naturally nontransformable, low-GC-content, Gram-positive bacteria. Appl Environ Microbiol 70:6887–6891. https://doi.org/10.1128/AEM.70.11.6887-6891.2004.
27. Arantes O, Lereclus D. 1991. Construction of cloning vectors for *Bacillus thuringiensis*. Gene 108:115–119. https://doi.org/10.1016/0378-1119(91)90495-W.